Preliminary test for radiation tolerant electronic components for the LHC cryogenic system.

J. A. Agapito[3], F. M. Cardeira[2], J. Casas[1], A. Duarte[3], A. P. Fernandes[2], F. J. Franco[3], M. J. Gil[3], P. Gomes[1], I. C. Gonçalves[2], A. Hernández Cachero[3], U. Jordung[1], M. A. Martín[3], J. G. Marques[2], A. Paz[3], A. J. G. Ramalho[2], M. A. Rodríguez Ruiz[1] and J. P. Santos[3].

[1] CERN, LHC Division, Geneva, Switzerland.
[2] Instituto Tecnológico e Nuclear (ITN), Sacavém, Portugal.
[3] Universidad Complutense (UCM), Electronics Dept., Madrid, Spain.

Abstract

The LHC accelerator will use about 1600 main superconducting magnets operating below 2K. The magnets temperature is a control parameter and its target accuracy imposes very severe constraints on both the sensing element and its signal conditioner. They will both be installed inside the tunnel, thus exposed to a relatively high neutron fluence and gamma dose. It is then crucial to understand the effects of radiation on the performance of the electronic components that will be selected for the signal conditioner. This paper presents data concerning the radiation effects on typical active and passive discrete electronic components. This is the first step toward building a radiation tolerant signal conditioner.

1. INTRODUCTION

The typical signal levels involved in the measurement of resistive type cryogenic temperature sensors are in the milivolt range, with measuring accuracy of about 0.5%, imposing the use of low-noise instrumentation amplifiers. These devices are usually fabricated in bipolar technologies that according to the literature may exhibit a significant degradation when exposed to the LHC tunnel environment. For 10 years of operation of the LHC machine the expected neutron fluence is $2 \cdot 10^{13}$ n·cm^{-2} and the gamma dose is 500 Gy.

In order to evaluate and design radiation tolerant electronic systems, irradiation campaigns are being performed both at the Portuguese Research Reactor, RPI (at ITN, Portugal) and at CERN. The investigated components include passive and active devices under normal operating conditions.

2. IRRADIATIONS AT ITN

For these experiments, the reactor is operated at a reduced power of 2.5 kW, so that the fluence of $5 \cdot 10^{13}$ n·cm^{-2} is reached in about 5 days, with 14h operation + 10h stand-by per day. The components under test were mounted on several PCBs, placed inside a hermetic Al cylindrical container, immersed in the reactor pool. The container is lined internally by 1mm of Cd (to cut thermal neutrons) and surrounded by a 20mm thick Pb shield (to reduce the fission gamma field). It is placed in front of the reactor core, with its longitudinal axis perpendicular to the reactor face.

The neutron fission fluxes were measured with Ni detectors placed at the centre of the boxes that contained the PCBs. They are based on the averaged neutron cross section for the reaction $^{58}Ni + n \rightarrow {}^{58}Co + p$ in a ^{235}U fission spectrum. Figure 1 shows the measured flux distribution along the container's axis, as a function of the distance from each box to the container's inner face closest to the reactor core. A photodiode sensitive to neutrons was placed in one of the boards, so that the neutron fluence was monitored online.

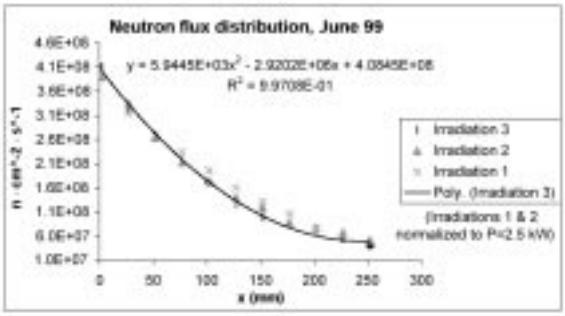

Figure 1: Neutron flux distribution

Gamma radiation both from fission and background origin is present when the container is immersed in the pool. Integration dosimeters placed on the back of each PCB reveal, after the completion of the tests, a total gamma dose between 17kGy and 3.5kGy.

Three campaigns have been performed, measuring passive and active components. Precision and standard thin film resistors, different types of capacitors, discrete active components and operational amplifiers were tested in the different periods. On-line measurements were performed by UCM before, during and after irradiation and stand-by periods, to evaluate the neutron and gamma irradiation damages as well as annealing effects.

2.1 Amplifier models and test set-up

Online measurements have been made on the following types of Amplifiers: Bipolar (OP27E, OP27F, OP77), JFET (TLE2071, LF351, LF356), DIFET (OPA111,

OPA124), LinCMOS (TLC2201) and Instrumentation (AD620, AD621, AD624). Figure 2 shows the proposed amplifier model [1], where:

- V+, V- and OUT are, respectively, the non-inverting input, the inverting input and the output voltages.
- V_{os} is the input offset voltage
- I_b is the input bias current
- I_{os} is the input offset current.
- R_{in} R_o are, respectively, the input and output resistances
- G_{ol} is the open loop gain, for operational amplifiers, or the externally controlled gain, for instrumentation amplifiers.
- CMRR is the common mode rejection ratio.

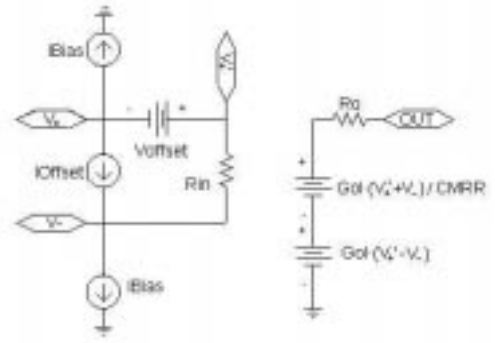

Figure 2: Operational Amplifier model

To measure the amplifier characteristics a standard test set-up is used [2], Figure 3. It permits online measurements of V_{os}, I_b, I_{os} and A_{vf} (closed loop gain). A set of electromechanical, relays remotely controlled, selects the adequate configuration to measure each parameter.

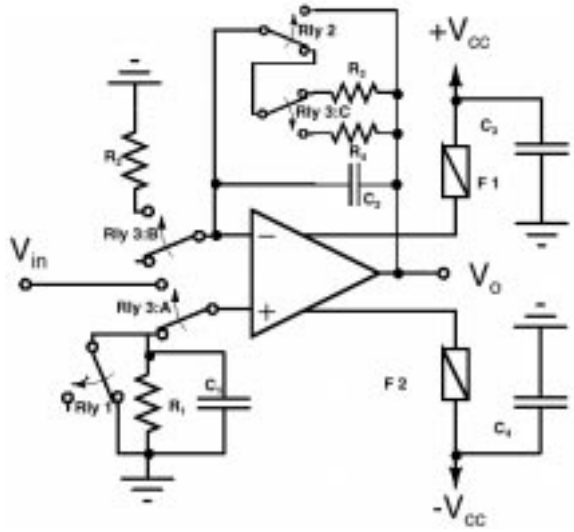

Figure: 3 Layout for Opamps parameters measurement

The PCBs inside the container are connected to the measuring system through a 20 m long shielded cable, with 50 twisted pairs of wires. Monitoring instrumentation incorporates an I-V source-measure unit, a digital voltmeter and a computer controlled switching system. A complete measurement cycle is performed every 20 minutes. The accuracy of measurements is 0.5% for A_{vf}, 1% for V_{os} and 5% for I_b & I_{os}.

2.2 Results

All the characteristics of the amplifiers changed with radiation. Their variation with neutron and gamma radiation depends on the fabrication technology. Moreover, some amplifiers are destroyed after ending the radiation exposure. There is a large reduction of open loop gain but adequate performance is observed for closed loop gains below 100.

Low frequency bipolar amplifiers (Table 1, Figure 4) show a linear growth of offset voltage up to a critical radiation dose, with an exponential annealing during stand-by periods. For higher doses, the offset voltage grows exponentially and the bias and offset currents degrade drastically

Table 1: Bipolar OP27E (Max. Tol. $1.16 \cdot 10^{13} n \cdot cm^{-2}$)

$n \cdot cm^{-2}$	**0**	10^{12}	$2 \cdot 10^{12}$	$5 \cdot 10^{12}$	$10 \cdot 10^{12}$	**max**
kGy	**0**	**.13-.26**	**.22-.48**	**.53-2.5**	**1.1–4.0**	**3.2 – 4.9**
A_{vf}	100.3	100.3	100.3	100.5	100.8	
	100.5	100.7	100.7	100.6	100.9	
	100.8	100.8	100.8	100.6	100.6	
	100.9	101.1	100.9	100.9	100.6	$1.65 \cdot 10^{13}$
	101.6	101.1	101.8	101	101.4	$1.16 \cdot 10^{13}$
	102	101.9	101.2	102	101.2	$1.83 \cdot 10^{13}$
$V_{os}(\mu V)$	-14	-410	-400	-290	-110	
	-19	-110	-90	-95	155	
	-17	200	370	820	1770	
	-20	10	-60	120	640	
	-20	40	80	430	1060	
	-10	130	230	140	160	
$I_b(nA)$	-20	360	1680	4630	7670	
	0	90	320	1040	1580	
	-5	120	340	820	1770	
	-10	630	1500	4420	6980	
	10	-20	-20	-30	-30	
	0	60	230	730	1250	
$I_{os}(nA)$	15	290	1380	3810	6290	
	0	-1	-1	-1	0	
	0	-11	-16	-14	6	
	-10	540	1280	3710	6230	
	0	20	40	50	50	
	0	50	60	70	50	

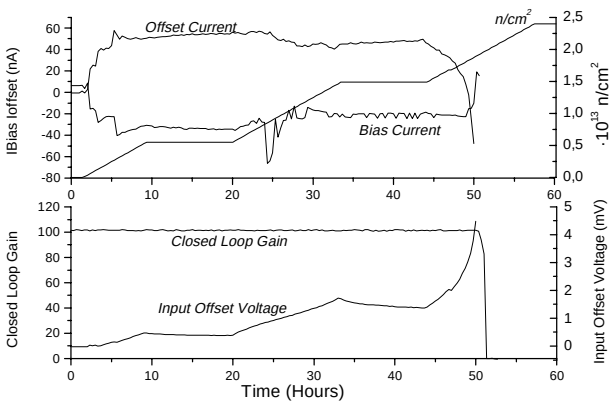

Figure 4: Bipolar operational amplifier

JFET input bipolar amplifiers (Table 2, Figure 5) show a variation in offset voltage that depends on the sample and its behaviour is not understood. Bias current grows parabolically, due to the variation of the carriers recombination time with the accumulated radiation [3]:

$$\tau^{-1} = \tau_0^{-1} + K \cdot \Phi(t)$$

The input current is that of a reverse-biased pn junction, thus:

$$I_b = I_{b0} \cdot (1 + k \cdot \Phi(t))^{1/2}$$

During reactor stand-by time, an exponential annealing is observed, reducing the bias current, that may be attributed to the partial vanishing of lattice defects. There is also a linear relationship between the bias current after annealing and the total accumulated dose.

Table 2: JFET TLE 2071 (Max. Tol. $3.5 \cdot 10^{13}$ n·cm^{-2})

n·cm^{-2}	**0**	**10^{12}**	**$2 \cdot 10^{12}$**	**$5 \cdot 10^{12}$**	**$10 \cdot 10^{12}$**	**$35 \cdot 10^{12}$**
kGy	**0**	**.13-**	**.22-.48**	**.53-2.5**	**1.1–4.0**	**6.6-7.8**
A_{vf}	99.6	99.8	99.5	99.7	99.4	
	100.5	100.7	100.8	100.6	100.6	
	99.6	100	99.8	100	99.7	
	100.3	100.1	100.2	100.9	100.3	100.3
	101.9	101.8	101.5	101.4	101.5	101.7
	100.5	100.1	100.2	100	100.8	
V_{os}(µV)	-370	-760	-870	-820	-1330	
	-160	-260	-430	100	430	
	230	540	570	250	-760	
	-70	-370	-420	-990	-830	-166
	20	240	110	190	-600	370
	-120	-390	-340	-390	-120	
I_b(pA)	-35	60	590	4850	34700	
	40	-80	710	9230	9640	
	-480	510	1090	6410	9810	
	600	-560	-100	2890	27260	387000
	630	-1720	-2270	-3210	-2530	-1230
	690	-1180	-1580	5280	59400	
I_{os}(pA)	5	350	320	280	-430	
	-120	940	870	990	1590	
	130	1190	1650	790	-60	
	-70	2020	2330	5110	3300	-970
	-50	2520	4250	5300	3450	1990
	-50	-4510	5850	4980	1780	

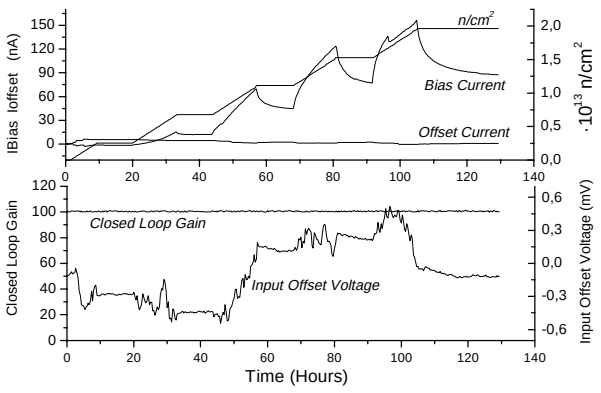

Figure 5: JFET Operational amplifier

DiFET amplifiers (Table 3, Figure 6) show an increase in offset voltage with radiation, but the variation is sample dependent. Gamma radiation is probably the origin of a fast variation in offset and bias currents initially due to positive SiO_2 trapping charge accumulation effects until they are compensated by the Si-SiO_2 interface charge generation for higher doses.

Table 3: DIFET OPA111 (Max. Tol. $3.3 \cdot 10^{13}$ n·cm^{-2})

n·cm^{-2}	**0**	**10^{12}**	**$2 \cdot 10^{12}$**	**$5 \cdot 10^{12}$**	**$10 \cdot 10^{12}$**	**$35 \cdot 10^{12}$**	**max**
kGy	**0**	**.18-.29**	**.27-.79**	**.61-1.8**	**2.0-3.5**	**2.6-6.0**	**8-11**
A_{vf}	100.4	100.5	100.6	100.5	100.3		
	100.4	100.6	100.6	100.6	100.3		
	99.8	99.9	99.8	99.8	100.2	100.1	
	100.9	100.7	100.6	101.2	101.2	101.5	$5.78 \cdot 10^{13}$
	100.9	101.4	100.9	100.9	100.7		$3.33 \cdot 10^{13}$
	100.6	100.2	100.5	100.2	100.6		
V_{os}(µV	520	2050	4530	8050	11600		
	160	-900	-1720	-3370	-5560		
	-160	590	1420	2400	4120	-8700	
	330	160	270	90	-1890	-34000	
	0	820	1190	2120	3480		
	30	1420	2070	4340	9120		
I_b(pA)	35	-190	-3780	-15	145		
	10	-20	820	-210	45		
	-10	390	730	2370	190	510	
	610	-1290	-5100	5680	-3550	-590	
	650	2860	-2340	4120	2500		
	600	-4050	-3400	-2100	-1010		
I_{os}(pA)	-10	1480	3870	320	180		
	10	210	210	660	440		
	-150	660	1310	1770	20	60	
	-70	2410	4020	5380	4950	3400	
	-50	4260	4420	5530	4860		
	-50	6240	5870	4920	3310		

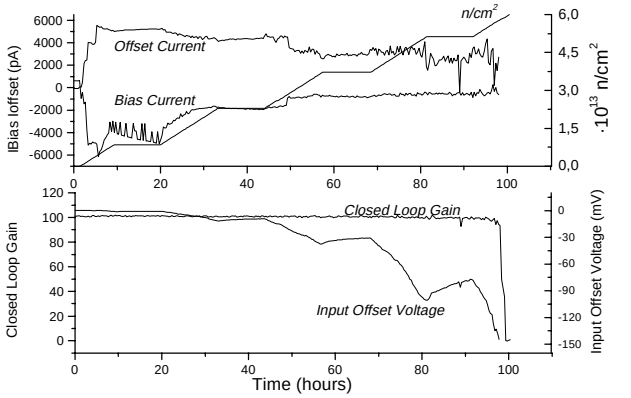

Figure 6: DIFET Operational amplifier

LinCMOS amplifiers (Table 4, Figure 7) increase their offset voltage with radiation. Offset current increases until reaching a fluence of $1.2 \cdot 10^{13}$ n/cm^2; where the current variation is inverted. Four of the tested samples were destroyed above $1.68 \cdot 10^{13}$ n/cm^2, probably due to the relatively high level of gamma radiation.

Table 4: LinCMOS TLC2201 (Max. Tol. $1.68 \cdot 10^{13}$ n·cm^{-2})

n·cm^{-2}	**0**	**10^{12}**	**$2 \cdot 10^{12}$**	**$5 \cdot 10^{12}$**	**$10 \cdot 10^{12}$**	**max**
kGy	**0**	**.13-.26**	**.22-.48**	**.53-2.5**	**1.1-4.0**	**3.7-6.4**
A_{vf}	100.7	100.9	101	100.2	100.8	
	99.4	99.4	98.3	99.1	94.4	1.810^{13}
	99.3	99.6	99.4	100.4	97.2	
	101.1	101.1	102	101.4	101.1	$3 \cdot 10^{13}$
	100.1	100	100	99.5	96.7	$2.68 \cdot 10^{13}$
	99.7	99.9	99.6	99.2	100.4	$1.68 \cdot 10^{13}$
V_{os}(µV)	-7	-240	100	2370	2600	
	5	710	2090	4690	15900	
	240	1090	1890	5830	13960	
	240	340	660	2210	4920	
	310	350	250	3040	9460	
	170	760	1610	5680	13480	
I_b(pA)	-380	12	-325	65	430	
	-300	-115	-350	100	475	
	2210	485	1010	3350	790	
	610	-1360	-1560	-1940	-2720	
	630	-1750	-2300	-2450	-2490	
	-60	-2030	-3200	-1870	-140	
I_{os}(pA)	2870	600	2350	9890	13970	
	3360	2730	6840	9990	6670	
	-2360	1320	2060	5590	6400	
	-790	2250	3170	9360	16900	
	1520	2600	4800	11500	22940	
	1720	4070	7300	15090	19500	

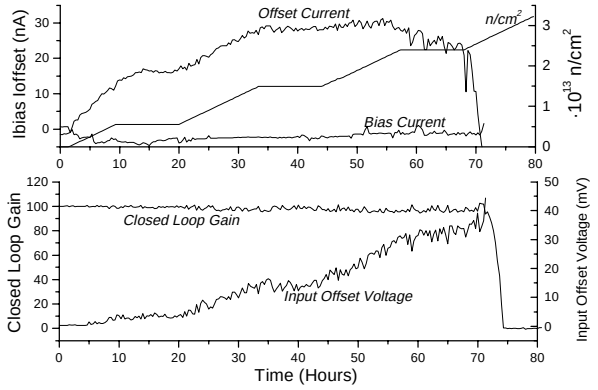

Figure 7: LinCMOS Operational amplifier

Instrumentation amplifiers AD620 and AD621 were destroyed at low neutron fluences below 10^{12} n·cm^{-2}. According to the literature much better hardness is obtained when using faster bipolar devices. This partially explains the good performance of AD624 (Table 5, Figure 8) that has better frequency characteristics. However one AD624 sample was destroyed at 10^{11} n·cm^{-2}.

Table 5: Instrument. AD624 (Max. Tol. $4 \cdot 10^{13}$ n·cm^{-2})

n·cm^{-2}	**0**	**10^{12}**	**$2 \cdot 10^{12}$**	**$5 \cdot 10^{12}$**	**$10 \cdot 10^{12}$**	**$35 \cdot 10^{12}$**	**max**
kGy	**0**	**.13-.20**	**.18-.32**	**.39-1.2**	**1.5-2.5**	**4.7**	**2.35**
A_{vf}	99.1	99.2	99.2	99.4	99.3		
	99.3	99.4	99	99.2	99.1	98	$4 \cdot 10^{13}$
	99.3	99.4	100.1	99.3	99.5		
V_{os}(µV)	-10	-140	-450	-830	-590		
	-80	-170	10	20	40	-324	
	0.12	0.09	0.12	-0.47	0.58		
I_b(nA)	-5	140	140	140	140		
	0	140	140	140	140	56	
	-70	-80	-80	-80	-80		
I_{os}(nA)	0	-10	-10	-10	-10		
	0	-5	-5	-5	-5	1	
	-70	-70	-70	-70	-70		

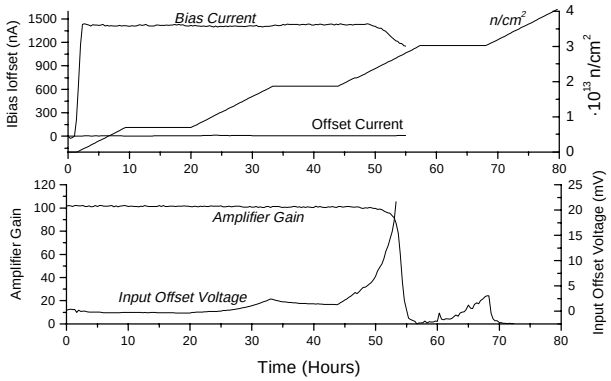

Figure 8: Instrumentation Amplifier

DC-DC converters, loaded at 40%, changed the output voltage linearly with radiation. During the stand-by period after radiation there was an exponential annealing, without recovering their initial value. Figure 9 shows the voltage variation of a multiple output dc-dc source as a function of temperature and neutron fluence.

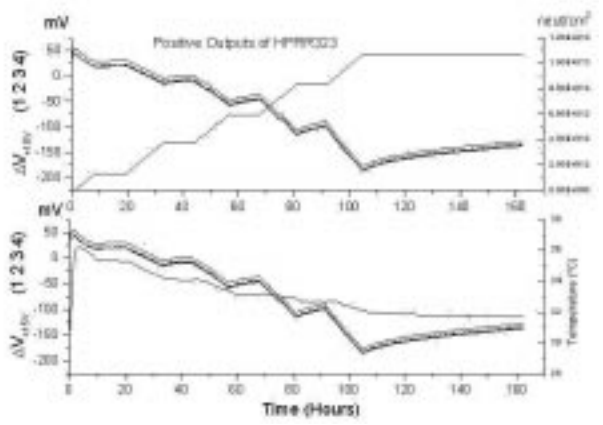

Figure 9: multiple output DC-DC converter

Thin film resistors, both high and ordinary precision types, are not affected by radiation and show a variation lower than 0.1%. Only some potentiometers exhibited a higher degradation, although below 0.7%.

3. IRRADIATIONS AT CERN

The CERN irradiation facility [4] is running in the TCC2 target area since May 1999, providing radiation levels of about 40 Gy/week + $1 \cdot 10^{11}$ n·cm^{-2} /week. After 17 weeks, roughly 650 Gy + $17 \cdot 10^{11}$ n·cm^{-2} have been accumulated.

Several units have been submitted to irradiation and monitored on-line once per hour. They comprise 5 boards with SMT passive components, of nominal values covering the range of interest, 12 signal conditioning units, a DC-DC converter and 3 voltage references. Ambient temperature is also monitored.

3.1 Test setup

The control and acquisition computer, measurement instrumentation and power supplies are installed in a control room 150m away from the irradiation area. The power input to each device under test is protected with a dedicated fuse, to avoid a general disruption of the supply in case of a latch-up.

In order to cope with the large number of readout channels, a multiplexing system was designed and installed near to the irradiated samples. It consists of 17 scanner cards, each sequentially selecting one out of ten 4-wire channels. Five cards are used to scan the passive components to be read from each board. Each of the remaining twelve cards is used to connect 1 out of 10 different resistors to each conditioner's input.

The design of the multiplexing system took into account the TCC2 radiation level. Each card is made out of ten 4-contact relays, driven by high-frequency bipolar transistors and selected by a modulo-10 CMOS counter. They are still fully operational.

3.2 Results

All resistors (2x 10 high-precision and 2x 7 ordinary-precision) and (2x 3) potentiometers survive 650 Gy + $17 \cdot 10^{11}$ n·cm^{-2} with no appreciable degradation ($\Delta R/R <$ 0.05%). Among 10 ceramic and electrolytic capacitors, some show a small initial drift and then stabilise at $\Delta C/C \approx 1\%$; others degrade less than 0.5%.

Two samples of ISOR-80-C ™ resistance to 4-20 mA signal conditioners, from Steiner Technik, show the gain increasing linearly with dose (600ppm/Gy), up to 200 Gy + $5 \cdot 10^{11}$ n·cm^{-2}. Above 250 Gy the output derives fast to saturation and becomes unusable.

Four samples of IPAC-L ™ resistance to 4-20 mA signal conditioners, from INOR show the output offset increasing linearly with dose (4μA/Gy), up to about 25-100 Gy + 0.7-2.6·10^{11} n·cm^{-2}. At this point, the gain drops to zero and the devices become unusable. However, one of the samples recovered but after a short irradiation period was definitely broken.

Two samples of IPAC-4L ™ resistance to 4-20 mA signal conditioners, from INOR, show the output offset increasing linearly with dose (-0.4μA/Gy), up to about 40Gy + $0.1 \cdot 10^{11}$ n·cm^{-2}. At this point, the gain drops slightly and the offset maintains the same behaviour until 100 Gy + $2.6 \cdot 10^{11}$ n·cm^{-2}, when the device is suddenly destroyed. Occasional ±6μA offset jumps suggest upsets in an 11.5bit ADC or DAC.

Two samples of LIN-multirange conditioners [5] are destroyed after 270 Gy + $7.1 \cdot 10^{11}$ n·cm^{-2} where the output drops to 4mA. One of the samples has 2 range-indicator optocouplers, which voltage decreases exponentially reaching -50% at 50 Gy + $1 \cdot 10^{11}$ n·cm^{-2}.

One sample of the T2F conditioner [5] show a degradation below 6%; the other sample had the output abruptly stopped at 40 Gy + $1 \cdot 10^{11}$ n·cm^{-2}, while internally operational; it recovered after 3 weeks annealing.

Two samples of LOG conditioners [5] show a degradation below 2.5%, difficult to distinguish from ambient temperature induced drift.

REF02 (5V reference) from BURR-BROWN, shows a drift of –6.3 ppm/Gy. REF02 (5V reference) from ANALOG DEVICES, shows a drift of +5.7 ppm/Gy. AD780 (2.5V reference) from ANALOG DEVICES, shows a drift of +2.5 ppm/Gy.

4. CONCLUSIONS

Instrumentation bipolar amplifiers like AD624 exhibit good radiation tolerance for neutron and gamma radiation levels expected in the LHC. DiFET and JFET amplifiers are in principle also good candidates; we believe that their relatively high degradation is produced by the gamma dose at ITN, that is significantly higher than for the LHC. Next experiments will be designed to discriminate between gamma and neutron radiation effects.

Also higher frequency bipolar devices will be tested, although a trade-off between radiation hardness and low frequency performance might be necessary. Fortunately, the high accuracy resistors have very good radiation hardness. It is thus possible to measure thermometric signals in a resistance comparison bridge, for reducing the effects of radiation on gain, offset and bias of the front-end analogue circuitry.

As could be expected, poor radiation performance is observed for industrial signal conditioners not intended to operate in a radiation environment. This is why we will continue with the evaluation of discrete components, to build all front-end electronics with parts fully qualified for the radiation levels expected in the LHC.

This work has been financed by the co-operation agreement K476/LHC between CERN & UCM and by the Spanish research agency CICYT (TIC98-0737), and partially supported by ITN.

5. REFERENCES

[1] "Analysis and Design of Analog Integrated Circuits" Third Edition, Paul R. Gray and Robert G. Meyer.

[2] "Burr Brown Operational Amplifiers Design and Applications". Jerald G. Graeme, Gene E. Tobey, Lawrence P. Huelsman. 1971.

[3] "The Effects of Radiation on Electronic Systems" Second Edition, G.e C. Messenger and M. S. Ash.

[4] "Electronic Components and Systems, Radiation Qualification for Use in the LHC machine", R. Rausch, Fifth Workshop on Electronics for the LHC Experiments, Snowmass, Colorado USA, 1999.

[5] "Signal Conditioning for Cryogenic Thermometry in the LHC", J. Casas, P. Gomes, K.N. Henrichsen, U. Jordung, M.A. Rodriguez Ruiz, CEC-ICMC'99, Monteal, Canada, 1999.